Geophys. J. Int. (2006) **165,** 817–834 doi: 10.1111/j.1365-246X.2006.02911.x

Hydroacoustic signals generated by parked and drifting icebergs in the Southern Indian and Pacific Oceans

Jacques Talandier,[1] Olivier Hyvernaud,[2] Dominique Reymond[2] and Emile A. Okal[3]

[1] *Département Analyse et Surveillance de l'Environnement, Commissariat à l'Energie Atomique, Boîte Postale* 12, F-91680 *Bruyéres-le-Châtel, France*
[2] *Laboratoire de Détection et Géophysique, Commissariat àl'Energie Atomique, Boîte Postale* 640, F-98713 *Papeete, Tahiti, French Polynesia*
[3] *Department of Geological Sciences, Northwestern University, Evanston, IL* 60201, *USA. E-mail: emile@earth.northwestern.edu*

Accepted 2005 December 21. Received 2005 December 17; in original form 2005 March 27

SUMMARY

We report the detection, principally by the French Polynesian seismic network, of hydroacoustic signals generated inside large icebergs, either 'parked' along the Wilkes coast of Antarctica in the Indian Ocean, or drifting in the Southern Pacific Ocean between latitudes of 55° and 65°S, during the years 2002–2004. The signals can be classified into two very broad families, based on the nature of their spectra. A first group features prominently monochromatic signals, whose frequency can, however, fluctuate with time during a single sequence of emission (typically lasting a few to a few tens of minutes). Such signals are generally reminiscent of those detected in 2000 in the Ross Sea and are generated principally in the Indian Ocean 'iceberg parking lot', between longitudes 144°E and 156°E. A new family of signals features a much broader spectrum, superimposed on a number of preferential frequencies suggesting the background activation of a number of resonators; these signals occur both in the parking lot and in the Southern Pacific. Further variations in spectra are documented inside each family. On the basis of similar *in situ* observations on Ross Sea icebergs under project SOUTHBERG, the first family is generally interpreted as expressing a stick-and-slip process during collisions between large iceberg masses. The second family of signals are observed during exceptional episodes of the otherwise silent drift of the icebergs in the deep Pacific Basin, some of which correlate with their passage over the various fronts defining the oceanographic southern convergence zone. Finally, a most recent episode of activity, generally similar to the above first family, was detected on 2004 December 3–4, at the ocean entry of the Dibble Ice Tongue, 600 km west of the parking lot along the coast of Antarctica. It is interpreted as resulting from collisions between large drifting icebergs and fragments of the ice tongue calved off during its disintegration, as documented by satellite imagery.

Key words: hydroacoustics, icebergs, Southern Ocean, *T* waves.

1 INTRODUCTION

In a previous contribution (Talandier *et al.* 2002; hereafter Paper I), we analysed hydroacoustic signals recorded as *T* phases in late 2000 by island-based seismic stations of the Polynesian Seismic Network [Réseau Sismique Polynésien; hereafter RSP] and originating from sources in the vicinity of Antarctica. Their spectral characteristics varied considerably, but usually featured prominent eigenfrequencies in the 4–7 Hz range, often accompanied by overtones. Over the duration of a sequence of activity (typically 2–10 min), the preferential frequency was observed to fluctuate slightly (by 10–20 per cent), often culminating in a slow upwards or downwards evolution upon the termination of the sequence.

Epicentral locations were obtained by combining Polynesian *T* phases with seismic phases interpreted as L_g and recorded both at the nearby VNDA station in Antarctica, and at stations of the Mount Erebus Volcano Observatory network deployed on Ross Island (Aster *et al.* 2001, 2004). The epicentres were found to correlate spectacularly well with the positions of massive icebergs, notably B-15B, detached from the Ross ice shelf in early 2000, and drifting in the central Ross Sea by the end of the year.

While the exact nature of the oscillator producing the hydroacoustic signal, as well as the mechanism of its excitation, remained speculative, we suggested that the former may involve a resonance either of the whole iceberg mass or of water-filled cracks in the ice sheet itself. As for the latter, we surmised that collisions between large ice masses drifting in the Ross Sea may act as triggers of the oscillators; this model gained support following the deployment of portable seismometers in 2003–2004 on iceberg C-16 and the recording of strikingly similar signals during documented episodes

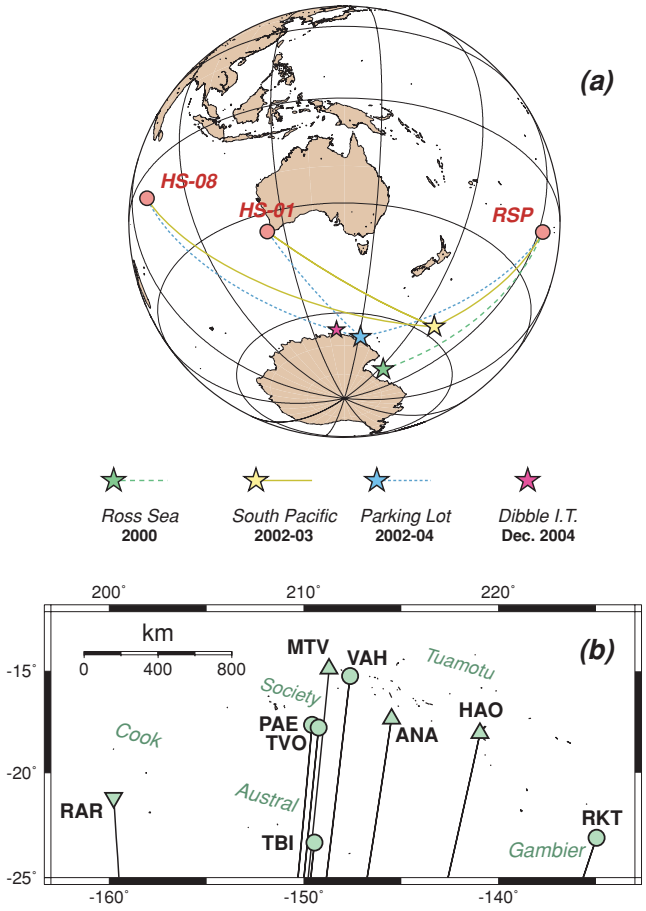

Figure 1. (a) General reference map sketching the relative position of the sources of cryosignals and of receivers used in Paper I and the present study. (b) Detailed map of receiver stations used in Polynesia (with codes). The names of the principal island chains are shown in italics. Circles identify permanent stations of the RSP and upward-pointing triangles temporary stations of the PLUME network; the downward-pointing triangle is the IRIS station at Rarotonga.

of collision and ramming of C-16 by another fragment of the original iceberg B-15 (MacAyeal *et al.* 2004). An alternative trigger could involve scraping against bathymetric irregularities in the continental shelf of the Ross Sea, whose depth may be locally comparable to the thickness of the floating ice sheets, estimated at ≈300 m.

In this general framework, the present paper reports a much enlarged data set of 'cryosignals', that is, hydroacoustic signals originating in icebergs, mostly drifting farther North in the Southern Pacific, in the 50°–65°S latitudinal band, or 'parked' in the vicinity of the Wilkes Land coast of East Antarctica (Fig. 1a). These events offer a variety of spectral characteristics, some of them duplicating the resonant features of the 2000 Ross Sea series, and others showing more complex spectra, requiring a different nature of acoustic source.

2 DATA SET

Since our initial identification of cryosignals in Paper I, a large number of additional observations have been reported (Talandier *et al.* 2003; Pulli *et al.* 2004; Chapp *et al.* 2004), using both land-based seismographs and the new hydrophone stations currently being deployed as part of the International Monitoring System of the Comprehensive Nuclear-Test Ban Treaty (e.g. Lawrence 1999). In this framework, it is rapidly becoming impossible to fully catalogue all observations of cryosignals, and the present paper has no pretence of completeness in this respect.

Rather, we focus here on some of the most spectacular and intriguing observations, most of them selected primarily on the basis of their amplitude, and reflecting the fluctuating detection and location capabilities resulting from variations in availability of data from various networks. The identification of hydroacoustic records as cryosignals proceeds from a combined assessment of their epicentral location, of their waveforms and, whenever possible, of the spaciotemporal correlation of their sources with the tracks of major icebergs, as documented from remote sensing.

Location procedure

Our location procedures have been previously described in several publications (Paper I; Reymond *et al.* 2003). Their algorithm is based on the propagation tables of Levitus *et al.* (1994), adjusted locally in the extreme southern part of the ocean, where a velocity of 1467 m s^{-1} is used south of 60°S, to reflect the disappearance of the SOFAR channel, and the rise of the layer of minimum sound velocity to the ocean surface. The validity of the algorithm was verified (north of the convergence zone) based on the recording at the Indian Ocean hydrophones of signals from the 2003 calibration experiment on board *R/V Melville* (D. Blackman, personal communication, 2003). As discussed in detail in Talandier & Okal (1996), the times inverted by the location procedure are not arrival times, which are usually difficult to pick on emergent phenomena, but rather differential times between stations obtained by cross-correlating their records.

All events discussed here were recorded at land-based stations of the RSP (Fig. 1b), principally VAH (on the atoll of Rangiroa), TBI and RKT (on the small coral-fringed islands of Tubuai and Mangareva) often complemented by PAE and TVO on the large island of Tahiti, and occasionally RAR (the IRIS station on the small reefed island of Rarotonga). In addition, we frequently used records from the portable stations operated as part of the PLUME network on the Polynesian atolls of Mataiva (MTV), Hao (HAO), and Anaa (ANA) (Barruol *et al.* 2002).

In general, events detected only at the Polynesian stations remain poorly located, with little control on epicentral distance. This results in elongated Monte Carlo ellipses (Wysession *et al.* 1991) (run with a standard deviation of Gaussian noise $\sigma_G = 1$ to 2 s) extending several hundred kilometres, and up to 1000 km if the extreme stations RAR or RKT are absent. Because of the small nature of the events, they were not recorded as seismic (or hydroacoustic) phases at the distant seismic stations in Antarctica which had constrained the 2000 epicentres at much shorter ranges [Paper I]. Such relatively poor locations will constitute a supplemental or 'secondary' data set of epicentres. Although only tentative in nature, their sources can nevertheless be valuable as they shed additional light on the origin of cryosignals.

The situation is quite different when data are available from the hydrophone stations deployed in the past few years at Diego Garcia (HS08) and Cape Leeuwin (HS01) in the Indian Ocean, as part of the International Monitoring System. As shown on Fig. 1(a), even one of these stations can provide crucial azimuthal coverage and the resulting Monte Carlo ellipses shrink to 20–30 km in semi-major

Table 1. Hydroacoustic relocation of documented Southern Ocean earthquakes.

Date	*T*-phase location			Reference epicentre			Relocation vector	
D M (J) Y	(°N)	(°E)	Origin Time	(°N)	(°E)	Source	Length (km)	Azimuth (°)
09 AUG (221) 2002	−62.03	154.36	11:43:51.6	−61.45	154.95	NEIC	72	205
28 AUG (240) 2002	−56.51	−142.72	21:09:28.9	−56.20	−142.72	NEIC	35	180
15 SEP (258) 2002	−59.12	−147.23	23:12:58.8	−58.98	−148.30	PIDC	63	105
11 OCT (284) 2002	−62.97	−160.70	13:48:48.1	−62.62	−161.27	NEIC	49	144

axis. We will interpret this figure as characteristic of the *precision* of our locations, which can be taken as expressing the quality of relative relocations of events belonging to a common spaciotemporal cluster. Such locations constitute our 'primary' data set of reliable epicentres allowing definite correlations with the spaciotemporal location of giant icebergs.

On the other hand, in the absence of ground truth for any of our events, we cannot evaluate directly the *accuracy* of our locations. We investigated this problem by using *T* waves to relocate four 2002 earthquakes located on the Antarctic plate boundary, from the Eltanin Transform at 142°W to the Balleny fracture zone at 155°E. Our results, summarized in Table 1, show relocation vectors separating the seismic epicentres listed by the USGS PDE catalogue from the hydroacoustic ones with lengths of 35–72 km. We stress that this technique cannot yield more than an estimate of the possible accuracy or our locations, given that the actual sources of acoustic and seismic energy from earthquakes could be distinct (e.g. Johnson & Norris 1968); in addition, the PDE seismic epicentres themselves could be erroneous by a few tens of km, as inferred from various relocation studies (Engdahl *et al.* 1998; Okal & Langenhorst 2000). Finally, *T* waves generated by earthquakes and other marine sources have notoriously different wave shapes. The former often feature emergent spindles, expressing the complexity of the source-side seismic→acoustic conversion (Johnson *et al.* 1968; deGroot-Hedlin & Orcutt 1999; Yang & Forsyth 2003), leading to the possibility of more systematic errors in location. In this respect, the coupling of iceberg sources to the water column is certainly a simpler process than the generation of a *T* phase by an earthquake, which should lead to more accurate hydroacoustic locations than for earthquakes. Nevertheless, we will take the average length of our seismic relocation vectors (55 km), as an estimate of the possible accuracy of absolute Southern Pacific locations of cryosignals from data sets of hydroacoustic arrivals in Polynesia and at the Indian Ocean hydrophones. The quality of the associations between our epicentres and the position of icebergs (see below) suggests that this estimate is probably too conservative.

In this general framework, we study here signals emanating from several broad areas, principally the continental shelf off the East Antarctic coast (from 135°E to 160°E) and the far reaches of the Southern Pacific between latitudes 67°S and 55°S and longitudes 157°E and 146°W (Fig. 1a). Note that no hydroacoustic signals definitely originating from the Ross Sea itself were recorded in Polynesia since 2000 December. Tables 2 and 3 list events from the primary and secondary data sets, respectively. The events are numbered in the 100, 200 and 300 series to provide an indexing commonality with those studied in Paper I, and to allow for a possible future expansion of the data set.

3 CORRELATION WITH ICEBERGS

In this section, we use a space-based data set comprising both reported positions and captioned photographs of major icebergs to establish spaciotemporal correlations with a majority of the events listed in Tables 2 and 3. The Appendix further examines and refutes the possibility of either a volcanic or a tectonic origin for the signals under study.

Signals from the 'Parking Lot'

We first focus on the region grossly delimited by Latitudes 68°S and 66°S, and Longitudes 148°E and 155°E, which we will call the 'Parking Lot', as many mega-icebergs originally calved off the Ross Ice Shelf congregate there for extended periods of time (occasionally years), after crossing the Ross Sea and rounding Cape Adare. In particular, B-15B, the site of the original cryosignals described in Paper I, reached the Parking Lot in late 2001 and remained essentially stationary near 67°S; 151°E for most of 2002 and 2003, before breaking loose again around 2004 March and leaving the Parking Lot in the summer of 2004. As of 2005 March 4, it was about 72 × 37 km in size and drifting westward in the Southern Ocean, around 64.5°S; 136°E.

Other local sources of icebergs parked in the lot are the small Cook Ice Shelf (around 153°E) and the prominent Ninnis and Mertz ice tongues extending from the George V Coast of Antarctica, at Longitudes 148°E and 145°E, respectively.

As detailed in Tables 2 and 3 and Fig. 2, we located six primary events in the Parking Lot proper and two more (Events 105 and 106) around 66.0°S; 148.2°E, approximately 100 km to the northwest. In addition, we located nine secondary events in the same general area. Some of them (e.g. Event 156 on 2004 February 17), recorded by as many as seven RSP-PLUME-IRIS stations, have well constrained locations despite the absence of hydrophone records. Others, such as Event 154, have patterns of traveltimes to the few stations recording them compatible with the epicentres of better-located primary events. This is illustrated on Fig. 2, for example, by the very large and elongated Monte Carlo ellipse for Event 154, pointing in the direction of the RSP. Even though the formally inverted epicentre falls 140 km northeast of the limits of the figure, the ellipse clearly intersects many icebergs and approaches by less than 20 km the epicentre of the much better-located Event 156, occurring only 11 days later; in many instances, we have also verified a similarity in waveforms. On this basis, we regard those secondary events as having occurred in the Parking Lot. This is also the case of Event 13 studied in Paper I, which shares traveltime patterns with the more recent Events 105 and 106, and also waveform characteristics with Event 105.

The correlation of our sources with icebergs is investigated through the use of the Quick Scatterometer (QSCAT) data set, as documented in Fig. 2, on which a map of epicentres is superimposed on a sample satellite photograph of the region taken on 2003 November 5. While the icebergs were not stationary over the duration of the study, and adequate satellite coverage may not be available for every single event in Tables 2 and 3, the slow drifting of the large icebergs allows an acceptable interpolation of their

Table 2. Primary Data Set.

Event Number	Date D M (J) Y	Origin Time (GMT)	Epicentre Latitude (°N)	Epicentre Longitude (°E)	Number of stations	σ (s)	e_{Max} peak-to-peak at VAH (μm s^{-1})	Duration (s)	Proposed Iceberg correlation	Type of source
				Events at Wilkes Coast 'Parking Lot'						
101	05 DEC (339) 2002	18:38:18	−67.83	149.35	4	2.34	0.73	45		I
102	26 MAR (086) 2004	05:24:54	−66.94	148.33	6	0.36	0.22	250	B-9B	(A) & (D)
103	12 MAY (133) 2004	03:28:04	−67.03	150.61	5	0.22	0.09	650	B-15B	(B)
104	07 JUN (159) 2004	02:51:56	−66.64	151.18	6	1.13	0.83	90		(C)
				Towards northwest						
105	12 JUL (014) 2003	14:08:19.8	−65.97	148.22	7	0.43	0.67	180		(D)
106	01 DEC (335) 2003	07:53:53	−66.04	148.25	6	0.01	0.12	200		(C)
				Farther west, Dibble Ice Tongue						
107	04 DEC (339) 2004	00:08:05.4	−64.78	134.70	7	0.01	0.4	700	C-19B	(A)
108	04 DEC (339) 2004	02:20:28.9	−64.79	134.71	7	0.04	1.1	600	C-19B	(C)
109	04 DEC (339) 2004	18:18:01.2	−64.77	134.68	7	0.01	2.1	100	C-19B	(D)
110	04 DEC (339) 2004	19:41:08.7	−64.72	134.53	7	0.04	2.0	130	C-19B	(D)
				Events correlating with B-19 Loops						
201	11 NOV (315) 2002	10:17:33.1	−57.30	−169.80	5	0.87	0.50	1800	B-19	I
202	13 NOV (317) 2002	16:02:00.6	−56.95	−169.69	5	0.95	0.65	180	B-19	III
203	25 NOV (329) 2002	15:06:36.1	−56.96	−169.89	4	0.05	0.79	*	B-19	III, II
204	25 NOV (329) 2002	20:26:57.9	−56.80	−169.59	5	0.19	1.24	30	B-19	II
205	25 NOV (331) 2002	20:30:00.1	−56.77	−169.66	4	1.83	0.59	15	B-19	II
206	29 NOV (331) 2002	05:16:25.9	−56.83	−169.48	4	0.09	2.32	120	B-19	I/
207	12 DEC (346) 2002	05:29:09.6	−57.30	−171.16	4	0.56	1.60	45		II
208	12 DEC (346) 2002	11:04:12.9	−57.05	−170.58	4	0.09	1.30	550	B-19	I
				Other Events in South Pacific						
301	07 MAR (066) 2002	09:10:25.1	−62.33	156.45	8	0.84	0.91	600	X-3	I
302	18 MAR (077) 2002	08:01:46.1	−57.48	−155.74	11	0.37	2.55	1200	X-2	I
303	02 AUG (214) 2002	19:29:30.5	−59.95	−175.36	7	0.31	2.18	1200	X-1	I
304	13 SEP (256) 2002	03:41:16.7	−54.94	178.60	9	0.22	1.14	900		I
305	10 OCT (283) 2002	18:07:16.8	−56.18	−150.13	8	0.36	2.25	900		I
306	15 JAN (015) 2003	04:42:15.5	−56.45	−149.58	5	0.62	1.05	500		I

*Two sequences of 180 and 120 s, respectively, separated by 9 min.

locations. In this context, we associate five events with specific icebergs in Table 2. Because of the similarity of the records, we extend this association to all 'Parking Lot' events listed in Tables 2 and 3.

Finally, a recent puff of activity on 2004 December 3 and 4 included four primary events (107–110) farther west along the Clarie Coast of Antarctica. These relatively small events were recorded only by the Indian Ocean hydrophones and the RSP station VAH; we obtained locations approximately 50 km north of a feature mapped as the Dibble Ice Tongue on Fig. 3; the first three epicentres are undistinguishable, but the fourth one is removed about 10 km to the northwest. We interpret these cryosignals as involving icebergs having calved from the ice tongue following its disintegration in 2004 November or December. A full discussion is given in Section 5. In addition, on the same day, at least nine secondary events were detected only by HS01, and only their backazimuths could be estimated from the triad of hydrophones at that station. They suggest that Events 162, 165, 166 and 168 also originated in the vicinity of the Dibble Ice Tongue. The other five (160, 161, 163, 164, 167) may have taken place at other locations along the coastline of Wilkes Land. A parallel interpretation is suggested for Events 13, 105, and 106, which probably involved fragments of the Ninnis and Mertz Ice Tongues, that are documented to have calved major ice blocks in 2000 February.

The Southern Pacific

The second parts of Tables 2 and 3 list events detected outside the Parking Lot, in an area extending from 67°S to 55°S in latitude and from 157°E to 146°W in longitude, across the vast expanses of the Southern Pacific, during the time window 2002 March–2004 October; their epicentres are plotted on Fig. 4 in the regional plate tectonics context. While most events occurred in the southern part of the Pacific plate, the recent one on 2004 October 31 (Event 360) took place significantly to the southeast, well inside the Antarctic plate.

The B-19 loops

We similarly investigated the possible correlation of the Southern Pacific epicentres with the position of major icebergs using the QSCAT database of satellite-tracked iceberg locations. In particular, Fig. 4 shows the trajectory of Iceberg B-19 in our study area, from 2001 July to 2002 December. It calved off the Ross Ice Shelf on 2000 June 13, as an elongated sliver measuring 43 km in length by 7 km in width. Its trajectory was initially northwards, then to the northwest, parallel to, and approximately 200 km off, the coast of Wilkes Land, until 2001 November 24, when it reversed direction eastwards towards the Balleny Islands, then north across the

Table 3. Secondary data set.

Event Number	Date D M (J) Y	Origin Time (GMT) (†)	Epicentre Latitude (°N)	Epicentre Longitude (°E)	Type of source
	Events at 'Parking Lot' and further west along Wilkes Coast				
13	14 JAN (014) 2001	17:40:00.7	−65.97	148.22	(D)
151	20 JAN (020) 2003	19:16			I
152	24 JAN (024) 2003	21:42	−68.27	155.33	I
153	05 APR (095) 2003	11:07:59			I
154	06 FEB (037) 2004	11:08:57	−65.58	155.76	(D)
155	07 FEB (038) 2004	10:01:43			(A)-(B)
156	17 FEB (048) 2004	10:42	−67.18	148.46	(B)
157	22 FEB (053) 2004	15:27			(D)
158	22 FEB (053) 2004	15:52			(D)
159	04 JUN (156) 2004	17:14			(D)
160	03 DEC (338) 2004	23:24			
161	04 DEC (339) 2004	05:50			
162	04 DEC (339) 2004	10:10			
163	04 DEC (339) 2004	11:26			
164	04 DEC (339) 2004	13:02			
165	04 DEC (339) 2004	14:10			
166	04 DEC (339) 2004	15:56			
167	04 DEC (339) 2004	16:00			
168	04 DEC (339) 2004	16:29			
	Southern Pacific events correlating with B-19 Loops				
251	08 NOV (312) 2002	07:02			I or II
252	11 NOV (315) 2002	09:56			
253	11 NOV (315) 2002	10:24			I
254	11 NOV (315) 2002	10:37			I
255	11 NOV (315) 2002	10:55			I
256	12 NOV (316) 2002	12:21			
257	13 NOV (317) 2002	12:28			
258	20 NOV (324) 2002	17:27			I
259	25 NOV (329) 2002	15:16			II
260	27 NOV (331) 2002	04:55			II
261	05 DEC (339) 2002	18:59			I
262	05 DEC (339) 2002	22:29			
263	05 DEC (339) 2002	22:32			
264	14 DEC (348) 2002	19:58			I
265	04 JAN (004) 2003	23:12			I
266	12 JAN (012) 2003	18:42			I
267	16 JAN (016) 2003	05:54			I
268	17 JAN (017) 2003	04:50			I
269	18 JAN (018) 2003	09:36			I
270	18 JAN (018) 2003	20:54	−57.63	−167.17	I
271	21 JAN (021) 2003	19:14			I
	Other events in South Pacific				
351	20 APR (110) 2002	08:32	−62.	156.	I
352	20 APR (110) 2002	09:46	−62.	156.	I
353	31 AUG (243) 2002	09:15 (V)			II
354	20 OCT (293) 2002	08:00 (V)			I
355	30 OCT (293) 2002	06:06			I
356	10 NOV (303) 2002	19:48:12	−60.31	−170.81	I
357	27 NOV (331) 2002	05:50 (V)			I
358	29 JAN (029) 2003	05:29 (V)			I
359	27 MAY (147) 2003	00:06 (V)			I
360	31 OCT (305) 2004	08:13	−68.12	−146.70	(D)

†When the origin time cannot be reconstructed because of a large uncertainty on epicentral distance, the time at VAH is given and flagged by (V).

Pacific-Antarctic Ridge, and northeast towards 57°S, 170°W. At this point, B-19 spends nine weeks, from 2002 October 11 to December 16, describing two major loops (Fig. 5a). The first one is about 60 km in diameter, and is covered at an average speed of 80 mm s^{-1}, or 7 km day^{-1}; the second loop is larger (90 km in diameter), displaced 120 km to the north and covered at twice the speed (170 mm s^{-1} or 15 km day^{-1}). While no hydroacoustic events are detected during the first loop (late October to early November), a spectacular

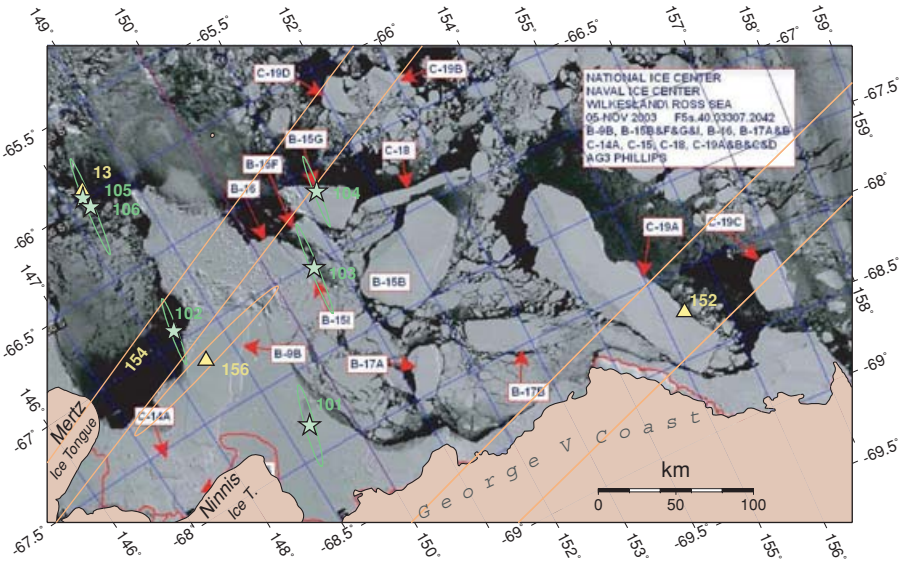

Figure 2. Map of epicentres in the Parking Lot, superimposed on a satellite photograph for 2003 November 5. Primary epicentres are shown as green stars, accompanied by Monte Carlo ellipses, and keyed to event numbers listed in Table 2. Triangles show epicentres from the secondary data set, listed in Table 3. Note extreme ellipses (orange) for those events.

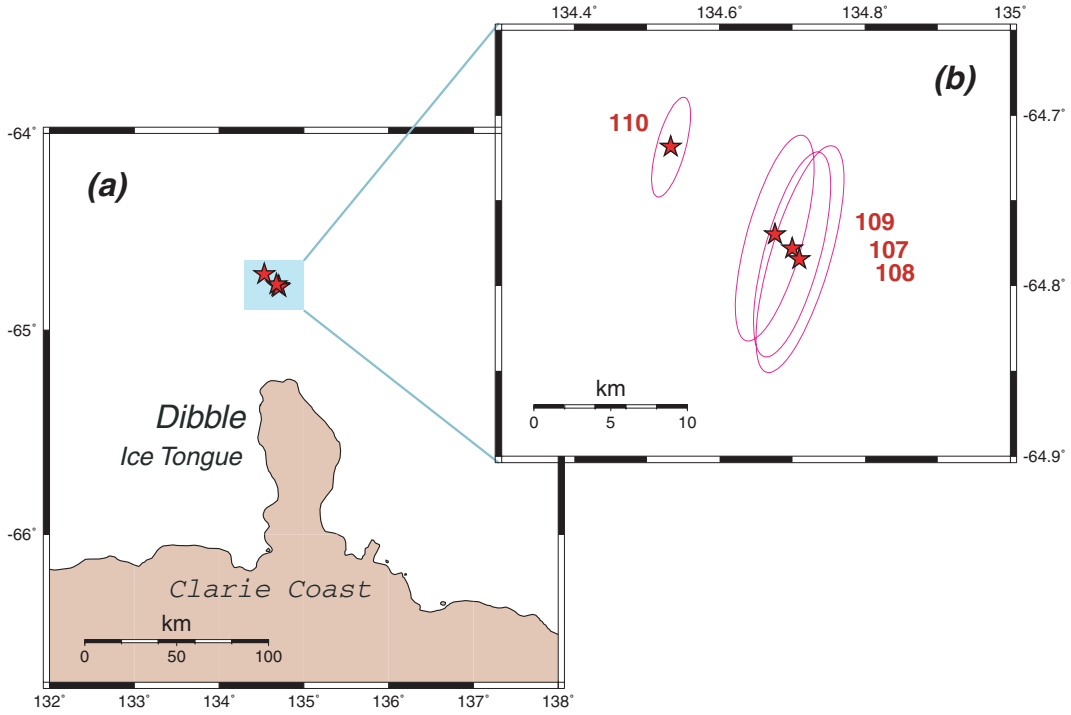

Figure 3. Location of cryosignals detected in 2004 December in the vicinity of Dibble Ice Tongue (see Fig. 1 for general location). (a): Epicentral location in relation to Dibble Ice Tongue; (b): Close-up of epicentres and Monte Carlo ellipses suggesting the resolution of two separate source areas.

spaciotemporal correlation exists between the path of the iceberg after the first loop and the occurrence of the major hydroacoustic swarm from 2002 November 11 to December 12 (Events 201–208).

Fig. 5(b) compares our inverted epicentres with the position of B-19, interpolated at the relevant time from the QSCAT database, whose average but variable sampling rate is about 1 point per day. We note that the misfit vectors range from 15 to 45 km in length (occasionally less when taking into account the epicentral error ellipse), the latter being comparable to the dimension of the iceberg, and therefore allowing a formal association between the hydroacoustic source and the ice mass. Indeed, the November–December swarm constitutes the most intense period of hydroacoustic activity in 2002–2004 in the Southern Pacific, and the B-19 loops are the largest irregularities in the whole drift of the iceberg, as mapped on Figs 4 and 5, suggesting that the coincidence of the two phenomena is not fortuitous.

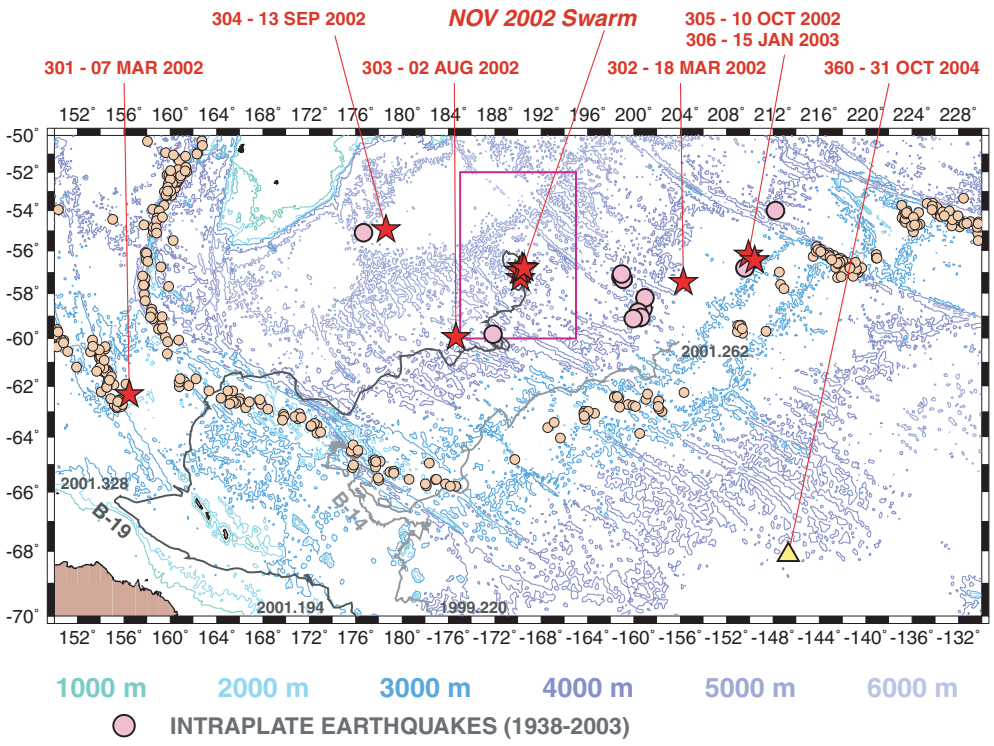

Figure 4. Bathymetric map of the Southern Pacific Basin, showing the location of the 2002–2004 activity. The plate boundaries are identified by the seismicity, as relocated by Engdahl *et al.* (1998), and plotted as small brown circles. The large violet disks are intraplate earthquakes from Wysession *et al.* (1991), updated to 2003. The stars identify primary epicentres from Table 2. Also shown (triangle) is the recent secondary event of 2004 October 31. The track of iceberg B-19 is plotted in dark grey, with Julian dates of its entry into the map, and western most excursion. The track of the silent iceberg B-14 is shown in lighter grey. The box outlines the region covered by Fig. 5(a).

In addition, it is probable that B-19 had spun off smaller icebergs, drifting in its vicinity but not catalogued in QSCAT; they may be associated with the more distant epicentre of Event 207, which we locate 55 km southwest of B-19.

Other South Pacific events

(1) *Event 303—2002 August 2*

Fig. 6 documents that a smaller unnamed iceberg(referred to here as 'X-1') is present only about 10 km from the uncertainty ellipse for Event 303. This iceberg is described as being 18 × 9 km (D. Long, personal communication, 2003), which allows a positive spaciotemporal association with Event 303. Note that X-1 took a sharp turn to the east only two days earlier.

(2) *Event 302—2002 March 18*

Similarly, an unnamed iceberg (referred to here as 'X-2') is documented about 16 km north of the Monte Carlo ellipse (Fig. 6b). This distance is only slightly greater than the reported size of the berg (12 by 12 km), which suggest a correlation. We do not have information on the kinematics of X-2's drift in the neighbouring days.

(3) *Event 301—2002 March 7*

In the case of Event 301, Fig. 6 shows that yet another iceberg ('X-3') is present approximately 60 km northeast of the epicentre. This distance is larger than the combination of an estimated size for the location's error ellipse (shown on Fig. 6), and of the probable size of the iceberg (18 × 7 km). However, it falls within the range of accuracy suggested by our earthquake relocation tests, and we suggest that Event 301 occurred inside X-3, or perhaps, in a smaller, unreported iceberg, most probably calved off X-3. We note that the QSCAT database reports only icebergs greater than 10 nautical miles (≈19 km) in their longest dimension.

In conclusion, a significant fraction of our epicentres can be correlated with the spaciotemporal position of documented large icebergs, both in the Parking Lot, in the ice fragments resulting from the collapse of the Dibble Ice Tongue, and in the Southern Pacific Ocean, most spectacularly in the case of the B-19 loops. We extend this interpretation as cryosignals to the remainder of the data set.

4 PROPERTIES OF THE WAVEFORMS

The purpose of this section is to attempt a classification of the cryosignals detected from the Southern Pacific Basin and the 'Parking Lot'. Their waveforms feature a broad variety of spectral properties, some of them comparable to those described in Paper I, the other differing significantly. We emphasize that any such classification remains tentative, in that the various types described here represent end members of populations occasionally blending into each other. With this qualification in mind, we observe that the cryosignals can be separated generally into two families, the first one featuring prominent, clearly resolved, spectral lines, while the second one involves a much broader ('whiter') spectrum against which eigenfrequencies may be present, but only as a weaker signal. In very general terms, but with significant exceptions, the first family of signals emanates from the vicinity of the Antarctic coastline (Ross Sea or Parking Lot), while the second one originates from icebergs adrift on the high seas. Within each family, several classes of signals can be recognized. We label them with letters in

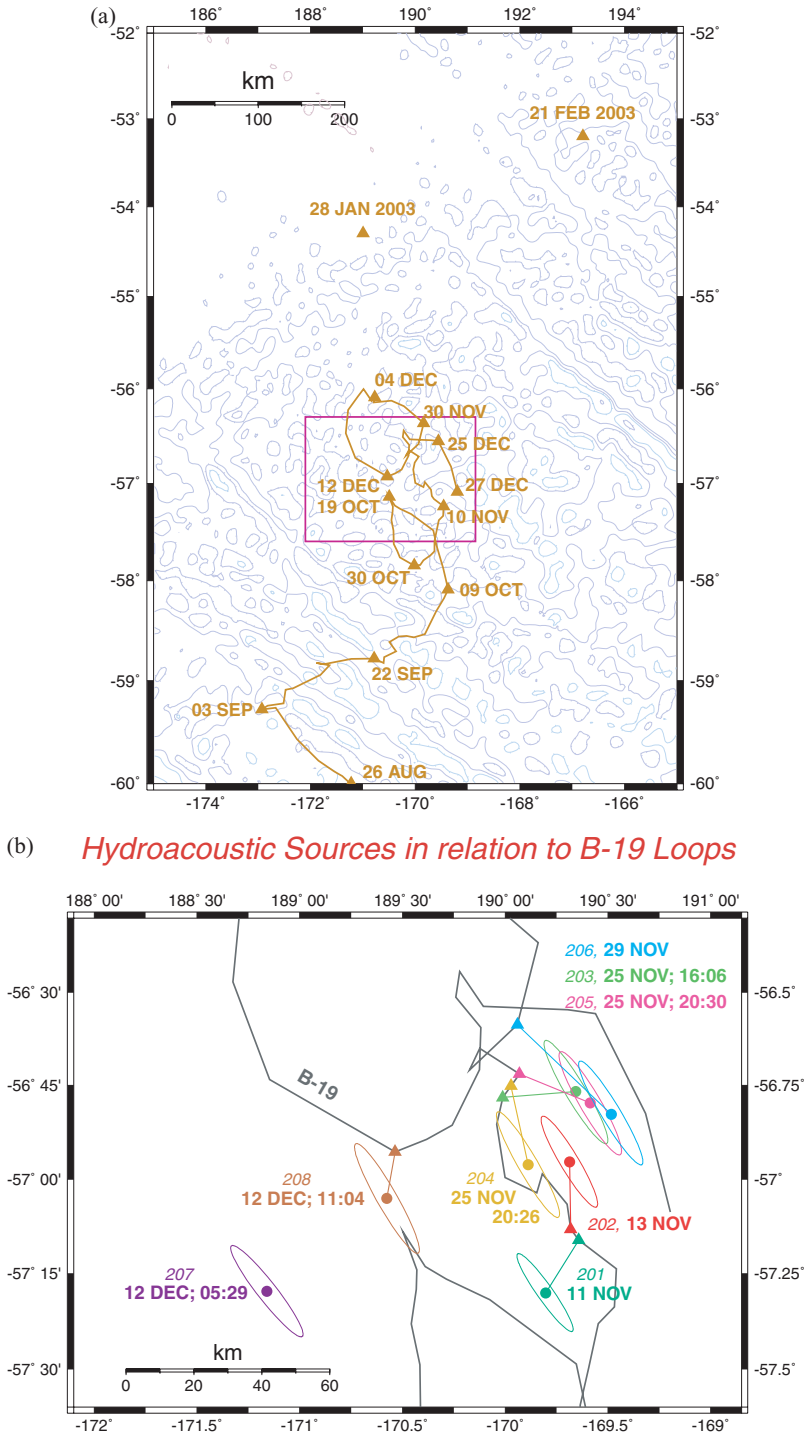

Figure 5. (a) Detailed path of B-19 in the last few months of 2002. Note the two loops travelled in October and December. The database stops on December 27, with two isolated reports in 2003. The box outlines the range of Fig. 5(b). (b) Close-up of Frame *a*, showing the path of B-19 between the two loops, and the primary epicentres listed in Table 2, together with their Monte Carlo ellipses. For each event, the position of B-19 at the origin time is shown as the triangle, linked by a solid segment to the epicentral estimate. Note that the iceberg is reported to be ∼40 km in length at that time. In the case of Event 207, we surmise that the source may belong to a smaller iceberg spun off from B-19.

the first family, and roman numbers in the second one, in order to preserve the possibility of further ramification of the classification in the future.

We start with the 2000 Ross Sea events described in Paper I, which could be separated into five general classes, to which many of the new events can be assigned.

(1) *Class (A):* Example: Event 3 (2000 November 12, 01:13; Fig. 1(b) of Paper I)

Such signals clearly feature a preferential frequency, but the spectral line itself is relatively wide and the spectrum noisy. When present, overtones are much weaker than the fundamental mode. During the ending phase of the signal, the eigenfrequency can evolve sharply,

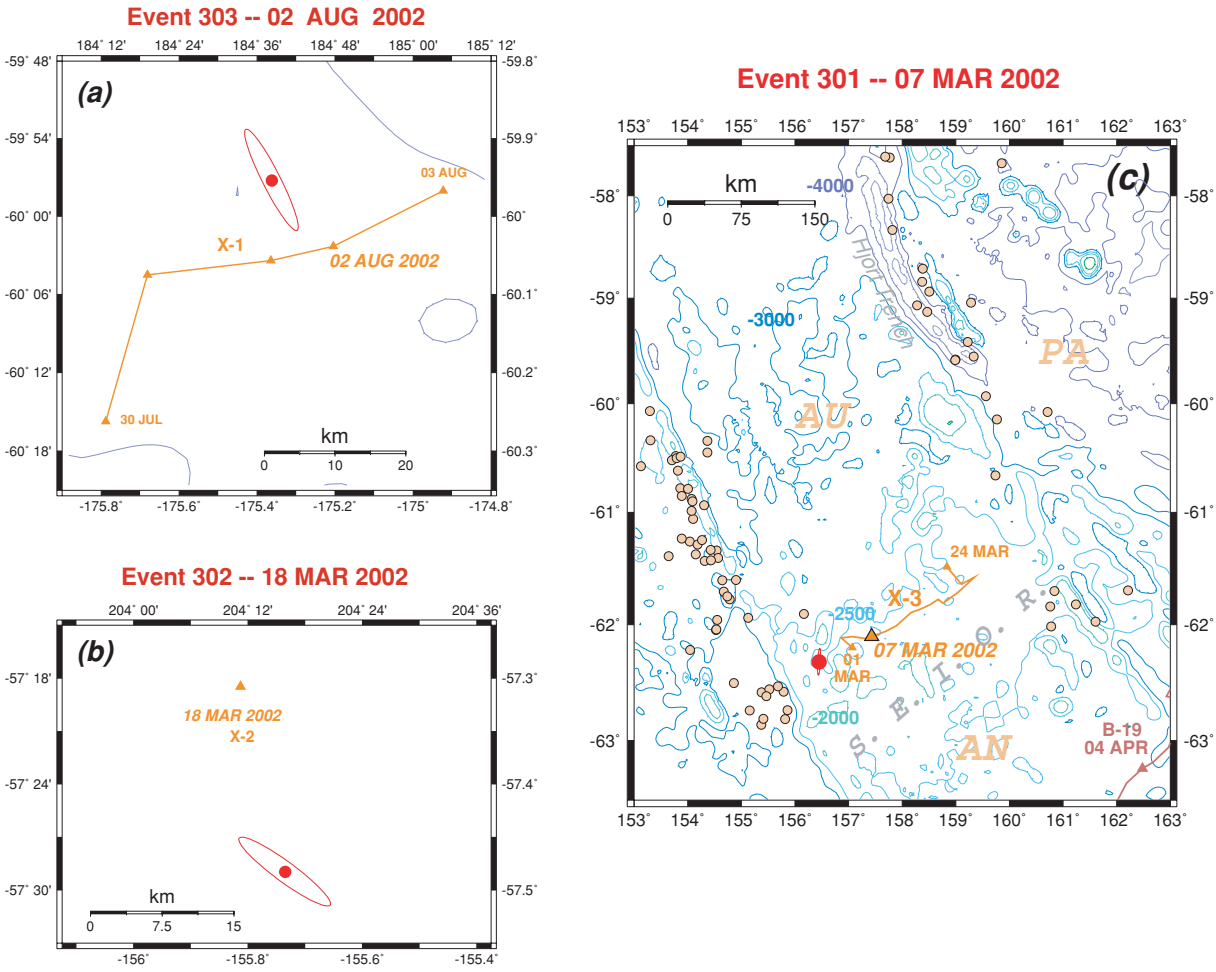

Figure 6. (a) and (b): Correlation of epicentres 303 and 302 (circles, with Monte Carlo ellipses) with Icebergs X-1 and X-2 (triangles), as tracked in the QSCAT database. The isobath on Frame (a) is at 4000 m. Note the sharp turn of X-1 about two days before the event. (c): Epicentre of Event 301 (solid dot, with small north–south Monte Carlo ellipse) in plate tectonics context. Open circles indicate background seismicity, delineating the junctions between the Australian (AU), Pacific (PA) and Antarctic (AN) plates. Also shown is the track of Iceberg X-3 during 2002 March, which was 60 km from the epicentre at the time of Event 301.

most often increasing with time, but occasionally 'gliding' down. Similar signals were documented from the Parking Lot, e.g. the early phase of Event 102 at Iceberg B9-B on 2004 March 26, and at the Dibble Ice Tongue (Event 107).

(2) *Class (B):* Example: Event 4 (2000 November 12, 06:00–09:00; Fig. 7a).

Signals featuring a remarkably monochromatic spectral line, with a high quality factor, usually accompanied by few, weaker harmonics. These sources can have a very long duration (3 hr for Event 4), during which the eigenfrequency may fluctuate as little as 10 per cent. Similar signals were observed at the Parking Lot, including Event 103 at B15-B on 2004 May 12, although it later evolved into a Class (D) signal. Fig. 7(b) shows another example at the Parking Lot, featuring an episode where the fundamental frequency of the oscillator is suddenly reset from a slowly decreasing value of 4 Hz to a significantly higher pitch (5 Hz), which then keeps increasing to a value of 6 Hz over a window of a few minutes.

(3) *Class (C):* Example: Event 2 (2000 November 8; Fig. 1(a) of Paper I).

These signals, characterized by a 'snake-shaped' spectrogram, represent a deterioration of Class (B), in which both the amplitude and frequency of the resonator fluctuate, the former to the extent of occasionally interrupting the oscillation, the latter over one or more octaves. Also, their duration is generally shorter than for Class (B). A spectacular example observed at the Parking Lot, Event 106 on 2003 December 1, is reproduced on Fig. 7(c). Event 108 at the Dibble Ice Tongue also featured the same behaviour during its early stages.

(4) *Class (D):* Example: Event 13 (2001 January 14; Fig. 1d of Paper I).

These events depart from Class (A) by being rich in overtones, and featuring a rapid non-periodic evolution of the eigenfrequencies, which can take a catastrophic character towards the end of a sequence (e.g. Event 13). A typical example at the Parking Lot is provided by Event 157 on 2004 February 22, reproduced on Fig. 7(d). Other occurrences of this class are Events 102 (early stage), 109, 158 and 360.

(5) *Class (E):* Example: Event 9 (2000 December 5; Fig. 1c of Paper I).

These signals feature a much broader 'noisy' spectrum, on which spectral lines are superimposed, with overtone amplitudes occasionally reaching those of the fundamental mode. Such signals were also recorded prominently when seismometers were operated directly on C-16 during the SOUTHBERG experiment (MacAyeal *et al.* 2004).

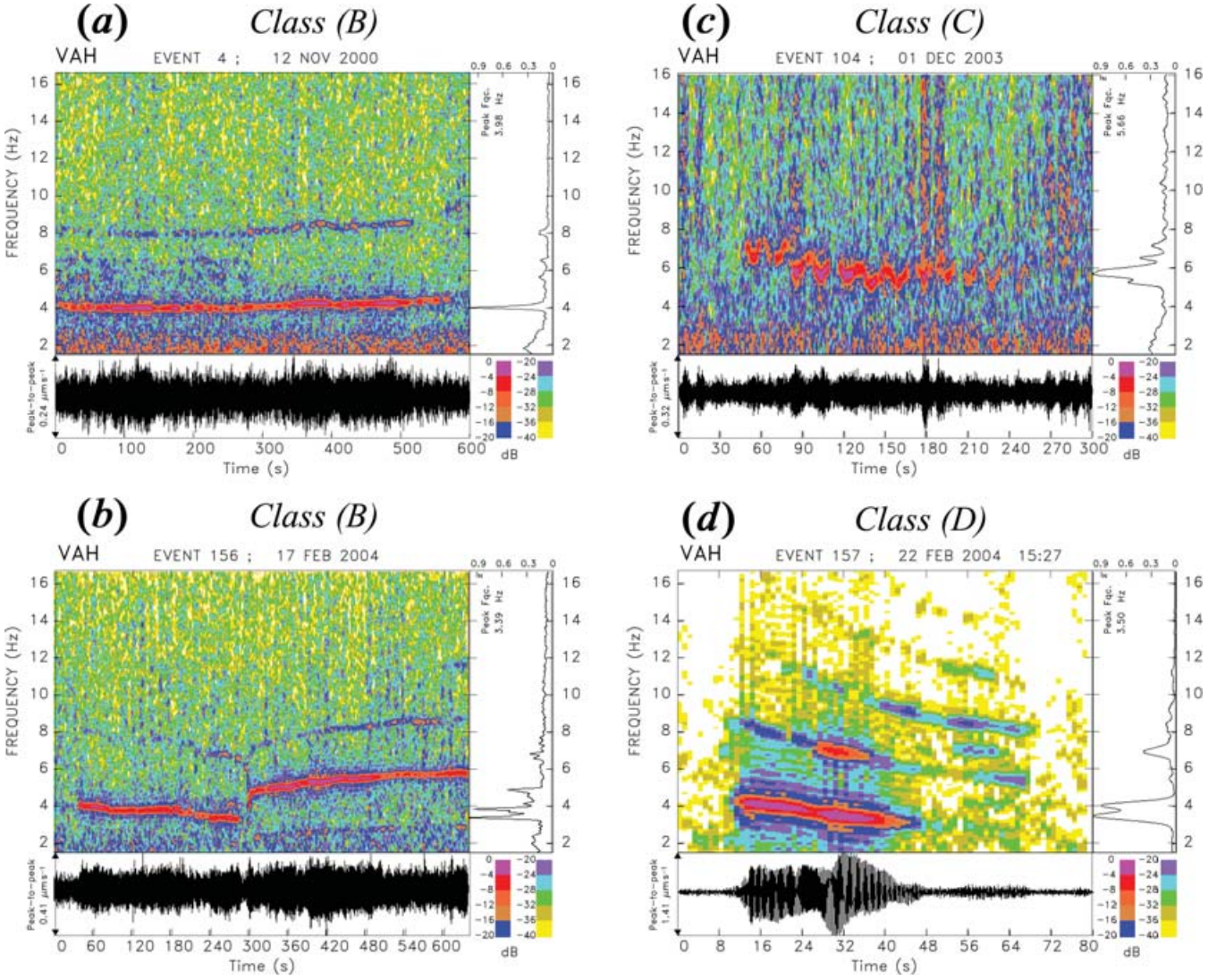

Figure 7. Spectrograms of various signals recorded at the RSP station VAH. We refer to Figures 1B and 1C of Paper I for examples of Class (A) and Class (E) signals, respectively. On each frame, the bottom trace is the original seismogram at VAH, high-pass filtered at 2 Hz (in the frequency range of a *T* phase, it is essentially a ground velocity record); the curve on the right panel shows the spectral amplitude of the record obtained through a simple Fourier transform; the main spectrogram diagram makes use of the Fourier Transform of a sliding window in the time series to illustrate the spectral amplitude present in the signal as a function of time (abscissa) and frequency (ordinate), colour coded using a scale in dB with respect to maximum spectral amplitude. Note the variable time scales. See text for details and interpretation.

Signals featuring a fundamentally broad spectrum include the following groups:

(1) *Cryosignal Type 'I':* Example: Event 201, 2002 November 11 (Fig. 7e).

This is by far the most common type of signal recorded throughout the new data set. It features an intense background noise, modulated in amplitude, but exhibiting preferential frequencies (e.g. around 5 and 7.5 Hz for Event 201 on Fig. 7e), which remain stable for the duration of the sequence. Superimposed is a succession of individual signals, of very short duration (typically a few seconds), featuring a broad, essentially white, spectrum extending past 10 Hz. The total duration of a sequence can reach 30 min. This type offers a great variability in the number of short signals emerging from the background noise, and in the relative signal-to-noise amplitudes. Instances of sharp, isolated signals with little if any background noise could constitute a sub-type (I′) of Type I, but the distinction between that category and regular Type I events is made difficult by an essentially continuous population.

Type I events were recorded from both the Parking Lot and the Southern Pacific Basin. With the exception of Event 360 (from the Antarctic plate section of the Southern Pacific; see above Class D), all isolated cryosignals originating in the Pacific (i.e. the individual, unrepeated signals in the 300-series) are of this type, as is the first event (201) in the B-19 loop series. Note also that similar signals were recorded directly on iceberg C-16, parked in the Ross Sea, during the SOUTHBERG experiment (Okal *et al.* 2004), which clearly affirms their origin as cryosignals.

(2) *Cryosignal Type 'II':* Example: Event 262, 2002 December 12 (Fig. 7f).

These less frequent signals differ from those of Type I in that the individual events last longer (up to 12 s), and are generally more emergent. Also, their spectra contain low frequencies, and are relatively discrete, i.e. featuring preferential eigenfrequencies. They

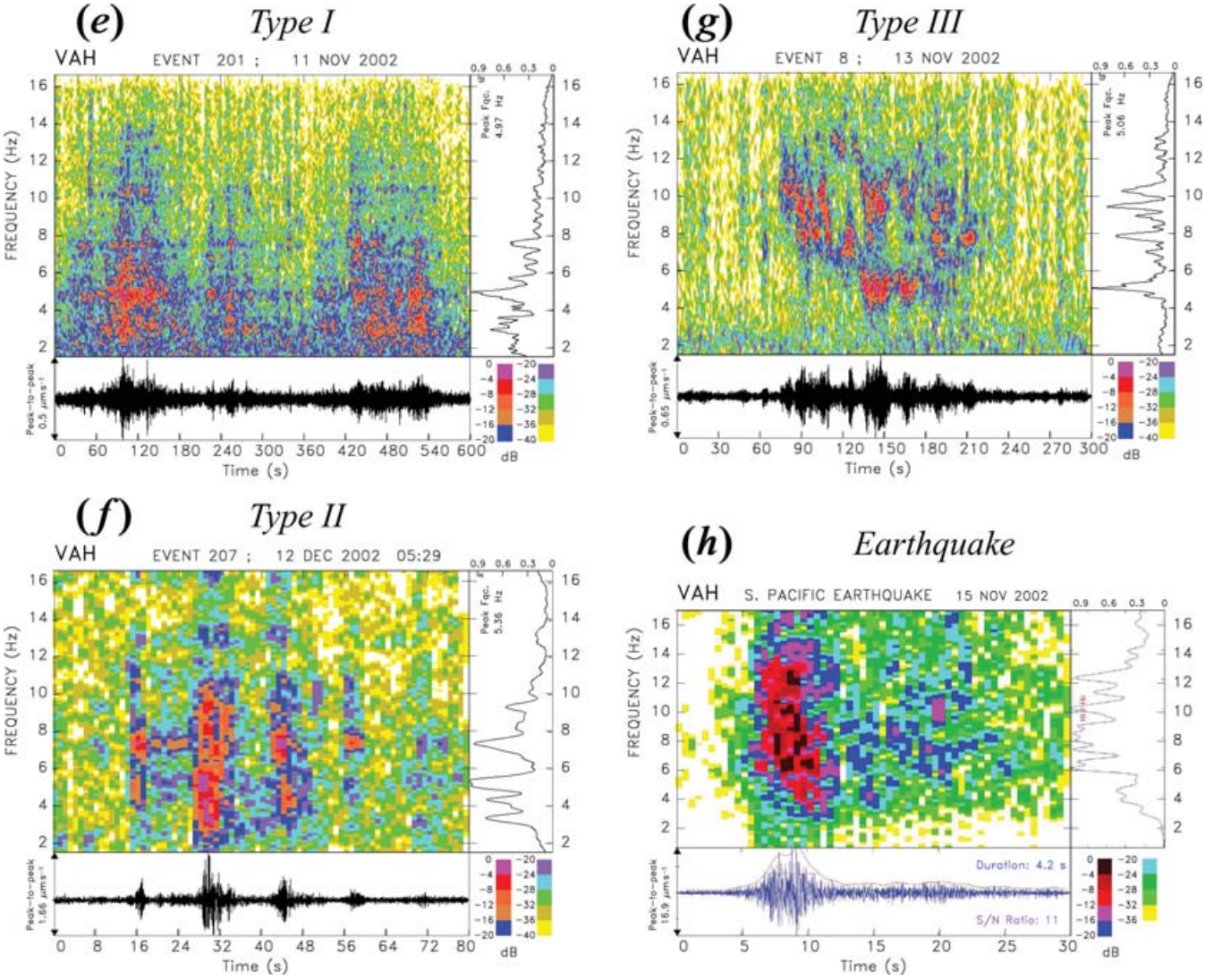

Figure 7. (*Continued.*)

were recorded occasionally both at the Parking Lot, and at the B-19 Loops.

(3) *Cryosignal Type 'III':* Events 202 (2002 November 13; Fig. 7g) and 203 (2002 November 25; 15:06)

These signals are characterized by a rapid succession of high-frequency events of short duration, featuring a relatively narrow spectrum built around readily evolving eigenfrequencies and their harmonics (Fig. 7g). As a result, in the frequency range recorded by the Polynesian stations (2–15 Hz), their spectrogram features the intriguing shape of a doughnut. We identified only two such cryosignals, but this rare pattern was tentatively recognized among the signals recorded during the SOUTHBERG campaign on Iceberg C-16 in the Ross Sea (Okal *et al.* 2004).

The two broad families of signals—mostly monochromatic (A-D) and featuring broad spectra (I–III) are essentially similar to the 'Variable Harmonic Tremor' and 'Cusp-Pulsed Tremor' described by Chapp *et al.* (2004) in their report on cryosignals observed at HS01 and HS08, and which they ascribe to events at (or close to) the Parking Lot.

(4) *Earthquake signals*

By contrast with cryosignals, we present on Fig. 7(h) a typical signal recorded at VAH from a presumed unreported earthquake. *T* waves from such sources feature a typical combination of a spindled envelope and a continuous generally low-frequency spectrum, expressing the complex source-side seismo-acoustic conversion involved with ridge or abyssal earthquake sources (Johnson *et al.* 1968; deGroot-Hedlin & Orcutt 1999; Yang & Forsyth 2003).

5 DISCUSSION

In reviewing the occurrence of cryosignals and attempting a discussion of their generation, we emphasize the difference between those featuring clear eigenfrequencies (even if the latter can fluctuate with time; typically of the (B) and (C) types), and those with a broader, more continuous spectrum (even if preferential frequencies can be present; typically Types I and II). In general, the former signals originate at continental margins, either in the Ross Sea in 2000, or in the Parking Lot since 2002, while the latter are generated on the high seas. This would suggest a different mechanism of vibration, and above all, of excitation. In particular, any mechanism involving interaction, such as scraping, with the ocean floor could

not take place on the high seas. However, there are exceptions to this simple classification, In particular, Type III (the 'doughnut' spectrum; Fig. 7g) has been observed both in the B-19 loops and during the SOUTHBERG project at Iceberg C-16 parked in the Ross Sea (Okal *et al.* 2004). Furthermore, Event 360, on 2004 October 31 is a unique occurrence of a superbly monochromatic signal apparently emanating from the high seas; its location is only secondary and hence tentative, but it is unlikely that it could be moved to the nearest continental shelf, more than 600 km to the south, along Ruppert Coast.

MacAyeal *et al.* (2004) have recently proposed that monochromatic signals recorded at C-16 may result from the development of a stick-and-slip process during episodes of collision between major ice masses. While C-16 has been restrained by the immediate presence of Ross Island and hence of very shallow water, such collisions had been documented over the continental shelf in conjunction with the 2000 events, during an episode of unimpaired drifting of B15-B at speeds comparable to those achieved over much deeper water [Paper I]. Thus, it would seem likely that similar collisions could take place over deep oceanic basins, such as in the epicentral area of Event 360.

In general, both Classes (A) and (B) are thought to be signals triggered during collisions between major icebergs, either as oscillations of fluid-filled cavities or as part of the stick-and-slip process involved by rubbing between the ice masses, as suggested by the *in situ* observations at the SOUTHBERG site (MacAyeal *et al.* 2004). Regarding Class (C), the period of frequency modulation of the oscillator remains remarkably constant during a given event, e.g. 50 s for Events 7 (2000 November 21; Ross Sea; Paper I) and 108 (2004 December 4; Dibble Ice Tongue), and 17 s for Event 104 (Parking Lot; 2003 December 1). Such periods have been found to be characteristic of background noise at seismic stations operated on Iceberg C16 as part of the SOUTHBERG project (Okal *et al.* 2004), and are in the range of the natural eigenfrequencies for bobbing, pitching and rolling of a thin ice layer averaging 300 m in thickness. The frequency modulation of Class C signals could thus represent an effect of such motions on the frequencies of yet unidentified oscillators.

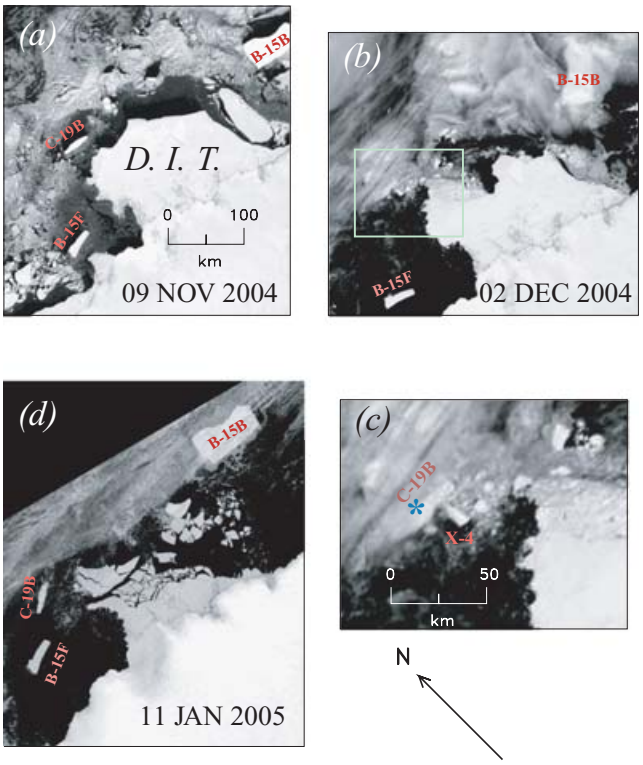

Figure 8. Collapse of the Dibble Ice Tongue (DIT) as documented by satellite photographs from the National Snow and Ice Data Center (time evolving clockwise from top left). (a): View of the Ice Tongue before the disintegration. Note the positions of icebergs B-15B, C-19B and B-15F. (b): Situation on 2004 December 2. The northern part of the ice tongue has started to disintegrate. Note the apparent rotation of B-15B. The green box outlines the area enlarged in (c). (c): Close-up of frame (b) around the epicentral region of Events 107–110 (shown as blue asterisk). Note the presence of the small ice tongue fragment X-4 (approximately 20 km long), suggesting an imminent collision with C-19B. (d): By 2005 January 11, the northern portion of the ice tongue has fully broken up, while C-19B has drifted farther west. Note that the projections used in the various frames are slightly different. For this reason, the scale bars on frames (a) and (c) are only tentative.

The case of the Dibble Ice Tongue

The Dibble Ice Tongue was a prominent structure extending about 70 km into the Indian Ocean from the Dibble Glacier, and mapped as part of the Antarctic Continent on Fig. 3. As documented on satellite images of the National Snow and Ice Data Center database (Fig. 8), it suffered a massive collapse between 2004 November and 2005 January. By 2004 December 2, the northern part of the Dibble Ice Tongue has started to disintegrate, and a small fragment (X-4) is approaching the larger iceberg C-19B (∼40 km × 8 km), drifting nearby, away from the Parking Lot area. By 2005 January 11, the northern half of the ice tongue has fractured, and by 2005 February 21, it is fully detached from the continental structure; however, by 2005 March 4, remnants of the ice tongue have apparently re-aggregated to form a narrower, tongue-like structure (Fig. 9).

Despite the rapid evolution of the ice structure between the various frames making up Fig. 8, and the slightly different (and unknown) projections used, we note the excellent correlation between our epicentral location for Events 107–109 (shown as the blue asterisk on Fig. 8c) and the position of C-19B only two days earlier. We thus surmise that Events 107–110 and the other activity on 2004 December 4 express the collision between the two ice masses, X-4 and C-19B. A most remarkable aspect of this interpretation is that hydroacoustic signals detectable in the far field were generated only during the collision, but not during the ice tongue collapse itself, even though its break-up and disintegration must have involved a large number of fractures over a time window probably lasting several weeks, based on the significantly different morphologies of the ice structures on Figs 8 and 9. Yet, the only signals detected at VAH were triggered during a 20 hr period correlated with the probable collision of X-4 and C-19B.

In this general context, we propose, tentatively, that Events 107–110 represent an evolutive sequence (Fig. 10), starting with a Class (A) event (107), triggered by the initial collision between X-4 and C-19B, followed by a modulated oscillation (Class (C); Event 108), and finally by the Class (D) Events 109 and 110, which are interpreted as resulting from rubbing of the two ice masses against each other.

Activity in the South Pacific Basin

Regarding cryosignal activity from the Southern Pacific Basin, we first observe that the transit of icebergs over oceanic basins is mostly silent. For example, Iceberg B-14 was a predecessor to B-19, which calved off the Ross Ice Shelf in 1999 and similarly drifted in the South Pacific during 2000–2001, albeit on a more southerly route

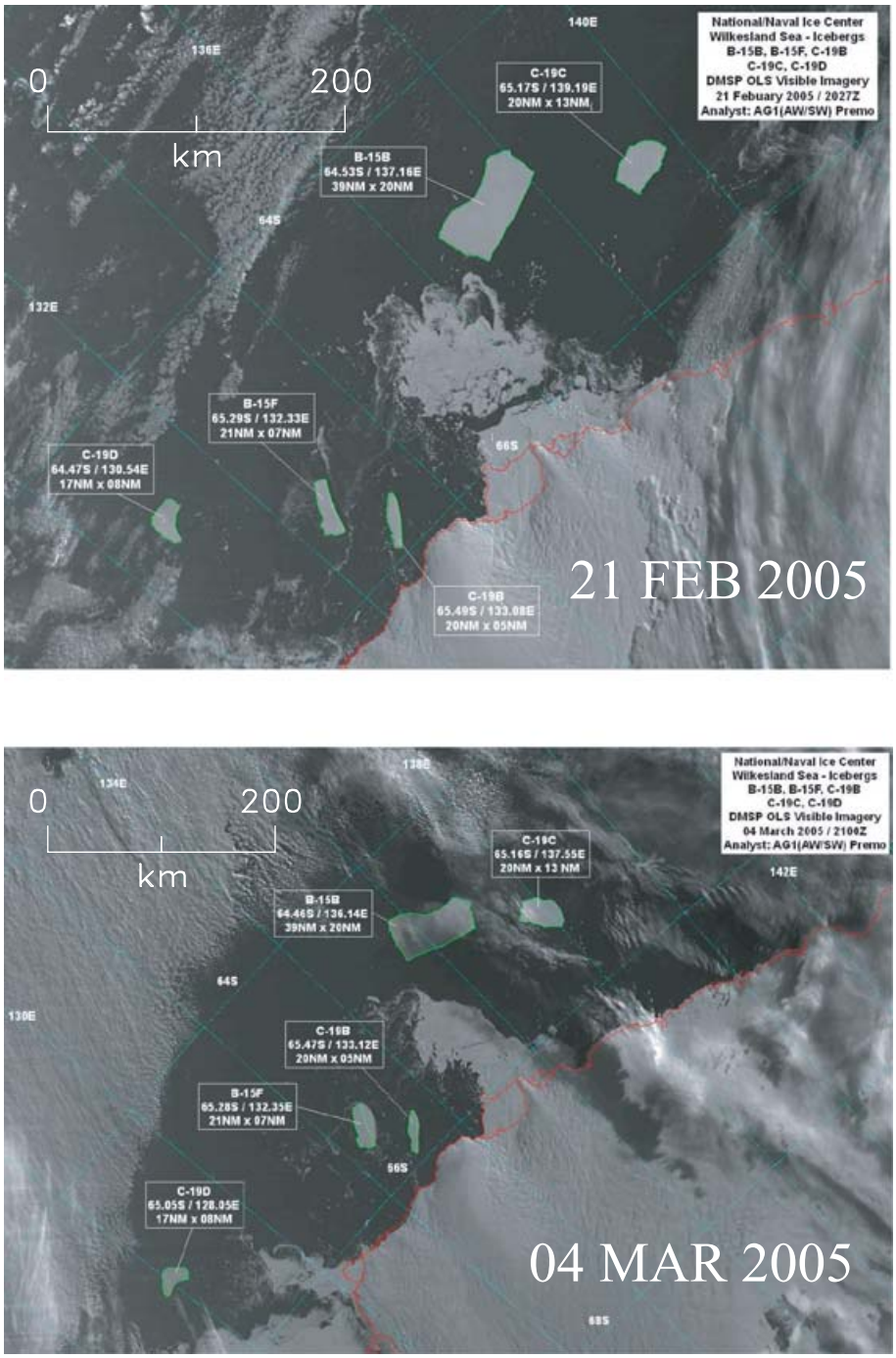

Figure 9. Further evolution of the Dibble Ice Tongue in early 2005, as tracked by the National Ice Center. On the top figure, the northern part of the ice tongue has disintegrated and is severed from the continental ice mass; however, on the bottom photograph, taken only 11 days later, a 70 km tongue has re-accreted. Note the different scales on the two frames.

(see Fig. 3). Yet, no hydroacoustic activity was detected at the RSP from B-14, even though its path involved a series of complex loops over the Pacific-Antarctic Ridge in 2000 July–September. As for B-19 itself, it had remained silent for more than a year before giving rise to the 2002 November series at the loops.

We must thus conclude that cryosignals are generated only during exceptional phases of the drift of icebergs on the high seas. The B-19 loops constitute an obvious example of turbulent kinematics, but the example of X-1 and perhaps X-3 (Figs 6a and c) would suggest that cryosignals can be emitted during, or immediately following, sharp and sudden changes in the direction of drift. In addition, we note that, with the exception of the B-19 loop series, most cryosignals emanating from the high seas are isolated in space and time.

The origin of the broader-spectrum cryosignals generated in the Southern Pacific Basin (Types I and II) is unclear. The presence of underlying preferential eigenfrequencies requires the activation of a resonator, and the fact that they usually do not fluctuate during the

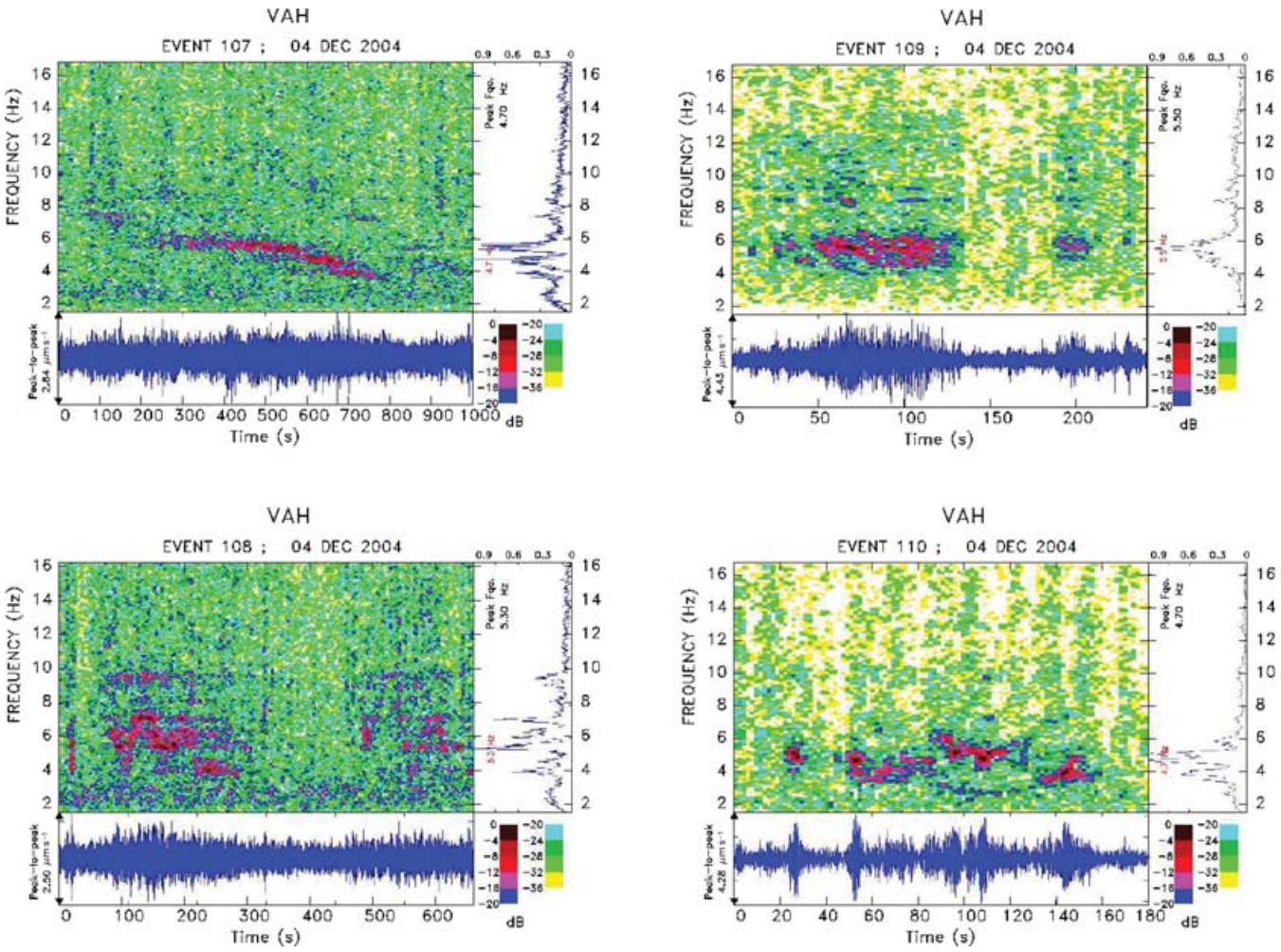

Figure 10. VAH spectrograms of Events 107–110 at the Dibble Ice Tongue. The series starts with a Class (A) event (107), followed by Event 108, whose initial part features the frequency modulation characteristic of Class (C), and by Events 109 and 110, which are more typical of Class (D). As suggested by Fig. 7(c), these events are most probably triggered by the collision between tongue fragment X-4 and drifting iceberg C-19B.

event would argue in favour of a mode of the entire structure. As for the nature of the triggering mechanism, it remains speculative, but several scenarios can be investigated.

Storms?

We discuss briefly the possibility that large meteorological perturbations could provide a mechanism triggering cryosignals in icebergs traversing them. The physical process would take the form of the accumulation of stress resulting from a lateral gradient in buoyancy forces across the ice mass under swells reaching amplitudes (10–15 m) comparable to the emerged height of the iceberg.

We have indeed been able to document large storms in the vicinity (tens to a few hundred kilometres) of acoustically active icebergs. However, no correlation can be established as stormy weather systems are ubiquitous in the Southern Ocean, with an average of five daily depressions mapped over the study area. In lay terms, the icebergs are drifting through some of stormiest seas in the world (known by sailors as the 'furious fifties' and 'screaming sixties'), where severe depressions occur on a daily basis, and do not constitute an exceptional encounter along their transit. Thus, we cannot propose that meteorological agents could be responsible for the relatively rare triggering of cryosignals.

The Polar Front connection

Rather, we think that the triggering of cryosignals in drifting icebergs may be related to their interaction with the oceanographic boundary generally referred to as the southern fronts. Fig. 11 shows that the epicentres under study are, with the exception of Events 301 and 360, all located between 60°S and 54°S. In the South Pacific, this is a region of rapid latitudinal variation in the physical properties of the Southern Ocean's waters (e.g. Nowlin & Klinck 1986; Orsi *et al.* 1995; Moore *et al.* 1999). It features two narrow transition zones known as the Polar Front and sub-Antarctic front (SAF). In simple terms, the Polar Front is a line of strong surface temperature gradients separating the Antarctic Ocean to the south (typically below 2°C) from the Polar Frontal Zone (which can reach up to 9°C), while the SAF, separating the Polar Front Zone from the sub-Antarctic Zone to the north, corresponds to a rapid change in the salinity profile of the ocean column. As a result, considerable mass exchanges take place in the region bordered by the Polar Front and sub-Antarctic Front, with the cold, dense waters of the Antarctic Ocean diving under their warmer neighbours to the north of the Polar Front.

The exact position of the fronts varies both longitudinally and seasonally and also features an erratic fluctuation from year to year.

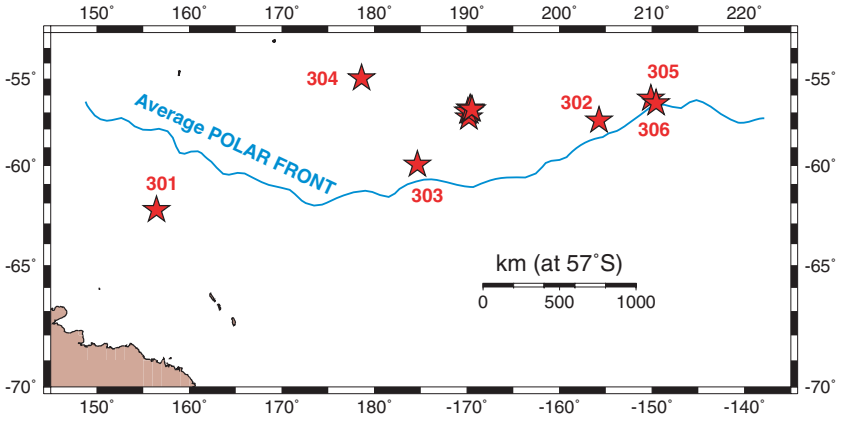

Figure 11. Epicentres of South Pacific Basin cryosignals in relation to the average position of the South Polar Front (solid line). The latter marks the boundary between the Southern Ocean and a zone of transition to the north, comprising the Polar Frontal Zone and sub-Antarctic zone, where most signals appear to originate.

Fig. 11 maps an average locus of the Polar Front across the Southern Pacific. A realistic latitudinal error bar for this boundary expressing both the existence of the several fronts and their fluctuation, would be +400 km (northwards) and −250 km (southwards). It is then clear that a good correlation exists between the Polar Frontal Zone, and the region of acoustic activity of drifting icebergs as mapped by hydroacoustic epicentres. A probable scenario involves the development at the Polar Front, and more generally in the Polar Front Zone, of a regime of complex surface currents characterized by the generation of intermittent eddies, which in turn are capable of entraining floating bodies such as large icebergs, thus explaining the B-19 loops. Again, one then expects a lateral gradient in the buoyancy forces acting on the ice structure, leading to a significant stress field inside the iceberg. We note in particular that the dimension of the iceberg (reported to still be in the tens of km) may be comparable to the scale of the eddies, as inferred from the size of the loops, but we can only speculate as to the exact mechanism by which oscillators (presumably related to cracks in the ice) could be triggered while B-19 was riding the eddies, and in particular between the two loops.

6 CONCLUSIONS

(1) We confirm that drifting or parked icebergs can be the source of intense hydroacoustic activity in the Southern Ocean, as first proposed in Paper I. However, we document a much more diverse set of signals, including families whose spectra are generally broader and for which preferential frequencies, when they exist, constitute more of a background trend than a primary characteristic of the spectrum.

(2) A most remarkable aspect of cryosignals is that they must correspond to exceptional phenomena involving the icebergs; most of the time the latter are silent during either their slow drift across vast expanses of the Southern Ocean, or their prolonged residence at largely stationary positions such as the Parking Lot. Similarly, the collapse of the Dibble Ice Tongue in 2004 November–December which resulted in its fracturation into a myriad of small ice masses (as documented by remote sensing from satellites) was not detected hydroacoustically.

(3) Thus, we suggest that cryosignals appear to occur only during catastrophic episodes of the transit of the icebergs. The Dibble Ice Tongue episode reinforces the suggestion, expressed in Paper I and by MacAyeal *et al.* (2004), that certain classes of cryosignals are generated by collisions between ice masses, with the preferential eigenfrequencies possibly triggered under a stick-and-slip process accompanying the rubbing of ice masses against each other, this tentative interpretation allowing the evolution or the modulation of the eigenfrequency during the collision process.

(4) By contrast, signals with a broader spectrum appear to be generated upon or immediately following significant variations in the kinematic parameters of the iceberg. These could be due to strong gradients in surface currents, which in turn could generate stresses due to gradients in buoyancy inside the ice masses. We note in particular that most events occurring in the South Pacific Basin (as opposed to close to the Antarctic shorelines) take place within the band comprising the Polar Front and the sub-Antarctic front.

(5) Finally, we wish to offer some perspective on the absolute amplitude of the cryosignals described in the present study. Table 2 shows that the largest signals reach $e_{\mathrm{Max}} \approx 2\,\mu\mathrm{m\ s}^{-1}$ as recorded on the atoll station at VAH at a typical distance of 60°. While it is difficult to interpret this figure in terms of an equivalent overpressure at or near the source, it is interesting to compare it to other natural and man-made *T*-wave signals recorded under similar conditions by RSP seismic stations. For example, we note that the two large presumed explosions off Oahu on 2000 April 13 reached only $0.30\ \mu\mathrm{m\ s}^{-1}$ (peak-to-peak) at Pomariorio (PMO) (Reymond *et al.* 2003; Fig. 2), at the shorter distance of only 37°. Similarly, routine seismic refraction campaigns off the coast of California were recorded on the northern coast of Rangiroa Atoll at $\sim 0.35\ \mu\mathrm{m\ s}^{-1}$ (peak-to-peak) (Okal & Talandier 1986) at a distance of 55°. The geometry of the receivers (a seismic station located within 100 m of the reef, along a shoreline directly perpendicular to the acoustic ray) is comparable in all cases. By contrast, earthquakes generate *T* waves recorded at levels routinely reaching 3 to 10 $\mu\mathrm{m\ s}^{-1}$ (zero-to-peak) (Talandier & Okal 2001; Fig. 6) and under exceptional circumstances up to 1 $\mathrm{mm\ s}^{-1}$, to the extent that such *T* waves have occasionally been felt by island residents (Talandier & Okal 1979).

In this respect, cryosignals constitute an additional source contributing energy to the hydroacoustic 'background' spectrum of the ocean at levels comparable to other natural sources, and significantly greater (typically by one order of magnitude in amplitude or two in energy) than those of many artificial sources, such as typical seismic refractions campaigns.

ACKNOWLEDGMENTS

We are grateful to David Long for guiding us through the QSCAT catalogue on the Bringham Young University website. We thank Guilhem Barruol for access to data from the PLUME network, and Doug MacAyeal for discussion. The paper benefited from reviews by Keith Koper and an anonymous scientist. This research was supported by Commissariat à l'Energie Atomique (France), and by the National Science Foundation, under Grant Number OPP-02–29492 to EAO. Maps were drafted using the GMT software of Wessel & Smith (1991).

REFERENCES

Aster, R., Mah, S.Y., Johnson, J., Kyle, P., McIntosh, W., Dumbar, N., Ruiz, M. & Desmarias, E., 2001. Seismic, acoustic and video observations of conduit processes during Strombolian explosions at Mount Erebus, Antarctica, *Eos, Trans. Am. geophys. Un.,* **82**(47), F1413, 2001 [abstract].

Aster, R. *et al.*, 2004. New instrumentation delivers multidisciplinary real-time data from Mount Erebus, Antarctica, *EOS Trans. Am. geophys. Un.,* **85,** 97 and 100–101.

Barruol, G., Debayle, E., Fontaine, F., Reymond, D. & Tommasi, A., 2002. PLUME: The French Polynesian upper mantle under study, *Eos, Trans. Am. geophys. Un.,* **83**(47), F1038 [abstract].

Chapp, E., Bohnenstiehl, D. & Tosltoy, M., 2004. Hydroacoustic observations of Antarctic-derived ice-generated tremor in the Indian Ocean, *Eos, Trans. Am. geophys. Un.,* **85**(47), F451, 2004 [abstract]

Chouet, B.A., 1992. A seismic model for the source of long-period events and harmonic tremor, in *Volcanic Seismology*, pp. 133–156, eds Gasparini, P., Scarpa, R. & Aki, K., Springer, Berlin.

Cole, R.H., 1948. *Underwater explosions*, Princeton Univ. Press, Princeton, New Jersey, 437 pp.

deGroot-Hedlin, C.D. & Orcutt, J.A., 1999. Synthesis of earthquake-generated *T* waves, *Geophys. Res. Lett.,* **26,** 1227–1230.

Dietz, R.S. & Sheehy, M.J., 1954. Transpacific detection of Myojin Volcanic eruptions by underwater sound, *Geol. soc. Am. Bull.,* **65,** 942–956.

Ekström, G., Nettles, M. & Abers, G.A., 2003. Glacial earthquakes, *Science,* **302,** 622–624.

Engdahl, E.R., van der Hilst, R.D. & Buland, R.P., 1998. Global teleseismic earthquake relocation with improved traveltimes and procedures for depth determination, *Bull. seism. Soc. Am.,* **88,** 722–743.

Géli, L. *et al.*, 1997. Evolution of the Pacific-Antarctic Ridge South of the Udintsev Fracture Zone, *Science,* **278,** 1281–1284.

Hyvernaud, O., Orzéa, J., Reymond, D., Talandier, J. & Okal, E.A., 2002. The 2001–2002 Volcanoseismic Swarm near Pitcairn Island, *Eos, Trans. Am. geophys. Un.,* **83**(47), F1050–F1051 [abstract].

Johnson, R.H. & Norris, R.A., 1968. *T*-phase radiators in the Western Aleutians, *Bull. seism. Soc. Am.,* **58,** 1–10.

Johnson, R.H., Norris, R.A. & Duennebier, F.K., 1968. Abyssally generated *T* phases, *Amer. Geophys. Un. Geophys. Monog.,* **12,** 70–78.

Lawrence, M.W., 1999. Overview of the hydroacoustic monitoring system for the Comprehensive Nuclear-Test Ban Treaty, *J. acoust. Soc. Am.,* **105,** 1037 [abstract].

Levitus, S., Boyer, T.P., Antonov, J., Burgett, R. & Conkright, M.E., 1994. *World Ocean Atlas 1994*, NOAA/NESDIS, Silver Spring, Maryland.

MacAyeal, D.R., Okal, E.A. & the SOUTHBERG Team, 2004. An *in-situ* investigation of the seismic symphony of Iceberg C16, Ross Sea, Antarctica, *Eos, Trans. Am. geophys. Un.,* **85**(47), F463 [abstract].

Molnar, P., Atwater, T., Mammerickx, J. & Smith, S.M., 1975. Magnetic anomalies, bathymetry and the tectonic evolution of the South Pacific since the Late Cretaceous, *Geophys. J. R. astr. Soc.,* **40,** 383–420.

Moore, J.K., Abbott, M.R. & Richman, J.G., 1999. Location and dynamics of the Antarctic polar front from satellite sea surface temperature data, *J. geophys. Res.,* **104,** 3059–3073.

Norris, R.A. & Johnson, R.H., 1969. Submarine volcanic eruptions recently located in the Pacific by Sofar hydrophones, *J. geophys. Res.,* **74,** 650–664.

Nowlin, W.D. Jr. & Klinck, J.M., 1986. The physics of the Antarctic circumpolar current, *Revs. Geophys.,* **24,** 469–491.

Okal, E.A., 1984. Intraplate Seismicity of the Southern part of the Pacific plate, *J. geophys. Res.,* **89,** 10 053–10 071.

Okal, E.A. & Langenhorst, A.R., 2000. Seismic properties of the Eltanin transform system, South Pacific, *Phys. Earth planet. Inter.,* **119,** 185–208.

Okal, E.A. & Talandier, J., 1986. *T*-wave duration, magnitudes and seismic moment of an earthquake, application to tsunami warning, *J. Phys. Earth,* **34,** 19–42.

Okal, E.A., MacAyeal, D.R., Stevens, S., Pančošková, P., Parker, T., Thom, J., Okal, M.H. & Aster, R., 2004. SOUTHBERG: Preliminary results of the operation of 4 seismic stations on Iceberg C-16, Ross Sea, Antarctica, *Eos, Trans. Am. geophys. Un.,* **85**(28), WP70 [abstract].

Orsi, A.H., Whitworth, T., III, & Nowlin, W.D. Jr., 1995. On the meridional extent and fronts of the Antarctic circumpolar current, *Deep-Sea Res. I,* **42,** 641–673.

Pulli, J.J., Upton, Z. & Bhattacharya, J., 2004. *T*-wave observations in the Indian Ocean, *Proc. NSF Workshop Seismo-Acoustic Applications in Marine Geology and Geophysics*, Woods Hole Oceanographic Institution [abstract].

Reymond, D., Hyvernaud, O., Talandier, J., & Okal, E.A., 2003. *T*-wave detection of two underwater explosions off Hawaii on April 13, 2000, *Bull. seism. Soc. Am.,* **93,** 804–816.

Sahabi, M., Géli, L., Plivet, J.-L., Gilg-Capar, L., Roult, G., Ondréas, H., Beuzart, P. & Aslanian, D., 1996. Morphological reorganization within the Pacific-Antarctic discordance, *Earth planet. Sci. Lett.,* **137,** 157–173.

Talandier, J. & Okal, E.A., 1979. Human perception of *T* waves: the June 22, 1977 Tonga earthquake felt on Tahiti, *Bull. seism. Soc. Am.,* **69,** 1475–1486.

Talandier, J. & Okal, E.A., 1982. Crises sismiques au volcan Macdonald (Océan Pacifique Sud), *C.R. Acad. Sci. Paris, Sér. II.,* **295,** 195–200.

Talandier, J. & Okal, E.A., 1984. New surveys of Macdonald Seamount, Southcentral Pacific, following volcanoseismic activity, 1977–1983, *Geophys. Res. Lett.,* **11,** 813–816.

Talandier, J. & Okal, E.A., 1996. Monochromatic *T* waves from underwater volcanoes in the Pacific Ocean: ringing witnesses to geyser processes?, *Bull. seism. Soc. Am.,* **86,** 1529–1544.

Talandier, J. & Okal, E.A., 2001. Identification criteria for sources of *T* waves recorded in French Polynesia, *Pure appl. Geophys.,* **158,** 567–603.

Talandier, J., Hyvernaud, O., Okal, E.A. & Piserchia, P.-F., 2002. Long-range detection of hydroacoustic signals from large icebergs in the Ross Sea, Antarctica, *Earth planet. Sci. Lett.,* **203,** 519–534.

Talandier, J., Hyvernaud, O., Reymond, D., Piserchia, P.-F. & Okal, E.A., 2003. Hydroacoustic signals from large icebergs drifting in the Southern Pacific, 2001–2003, *Eos, Trans. Am. geophys. Un.,* **84**(46), F356 [abstract].

Wessel, P. & Smith, W.H.F., 1991. Free software helps map and display data, *Eos, Trans. Am. geophys. Un.,* **72,** 441 and 445–446.

Wysession, M.E., Okal, E.A. & Miller, K.L., 1991. Intraplate seismicity of the Pacific Basin, 1913–1988, *Pure appl. Geophys.,* **135,** 261–359.

Yang, Y. & Forsyth, D.W., 2003. Improving epicentral and magnitude estimation of earthquakes from *T* phases by considering the excitation function, *Bull. seism. Soc. Am.,* **93,** 2106–2122.

APPENDIX

Could they be anything but cryosignals?

The spaciotemporal correlations between our epicentres and the positions of large drifting icebergs, as well as the spectral characteristics of some of the signals are the strongest evidence defining them as cryosignals. However, it is necessary to seriously examine—and refute—the possibility that they could be generated by other forms of activity not involving icebergs.

An obvious but important first observation is that, with the possible exception of Event 301, and given the precision of our method, the 2002 hydroacoustic sources cannot be placed on the various plate

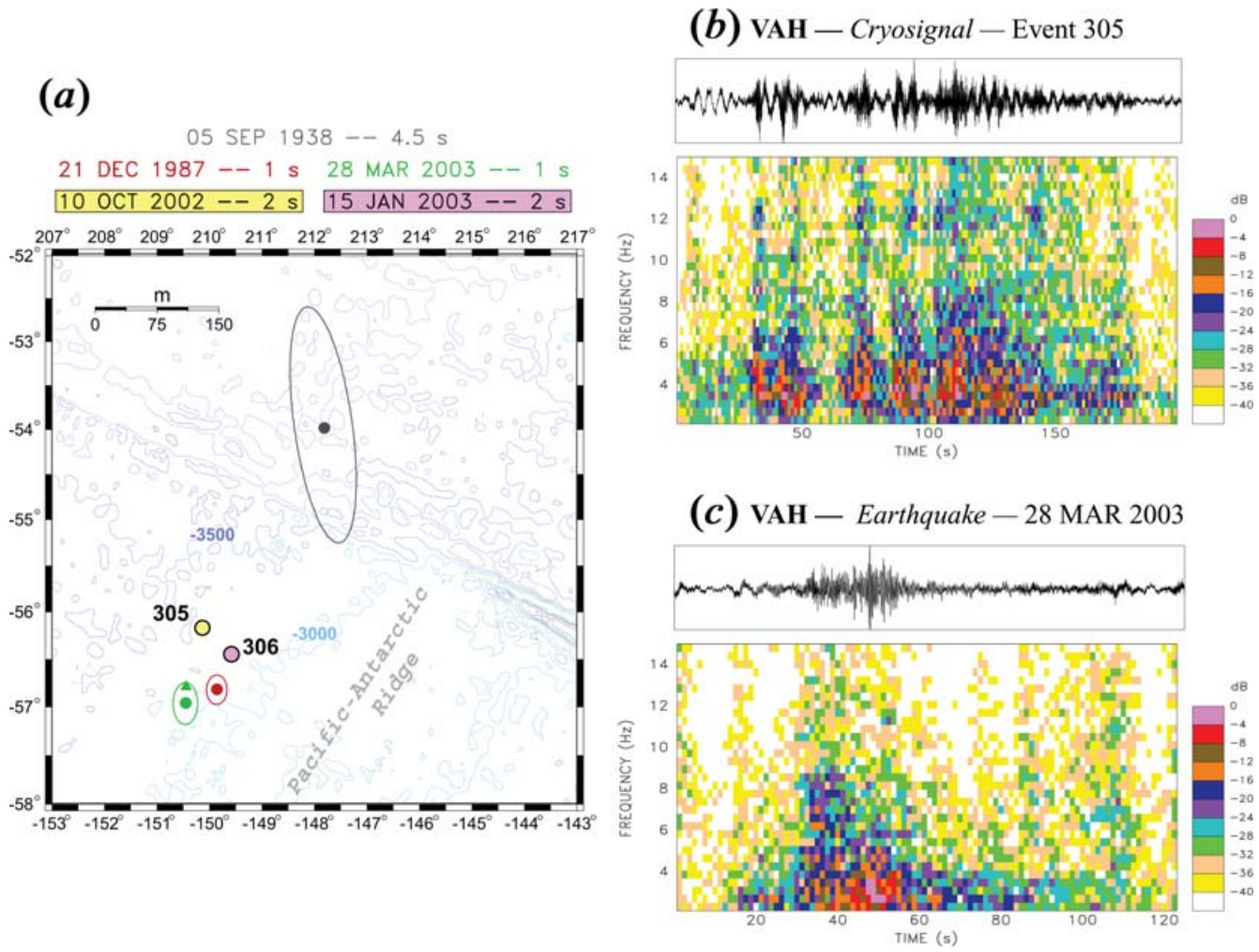

Figure A1. (a): Close-up map of the source region of Events 305 and 306. The colour-keyed solid symbols are relocated epicentres of local intraplate earthquakes. (The triangle is the preliminary USGS location of the 2003 event.) Monte Carlo ellipses (Wysession *et al.* 1991) are traced for Gaussian noise with standard deviations listed in the heading. The shaded open symbols are the epicentres of Events 305 and 306; their ellipses for $\sigma_G = 2$ s would fit inside the symbols. (b) and (c): Comparison of records and spectrograms at VAH for Event 305 (cryosignal) and for the 2003 earthquake. Note the different time scales.

boundaries. This rules out *prima facie* both volcanic activity at the mid-Oceanic ridges and earthquakes on their transform segments, as potential sources of our signals.

Volcanism?

Following the landmark study by Dietz & Sheehy (1954), hydroacoustic signals recorded at teleseismic distances have often been interpreted as volcanic in nature, and indeed many unsuspected abyssal volcanoes have been identified through *T* waves generated during their eruption (e.g. Norris & Johnson 1969). Having ruled out ridge volcanism as the source of the 2002 events based on their inferred location, we discuss here the potential case for intraplate volcanic activity. There exist some limited similarities between the 2002 signals and those of *T* waves of volcanic origin, namely the recurring superposition of individual intense sequences on top of background noise. However, these are clearly outweighed by significant disparities, which lead us to dismiss volcanism as a possible source of the 2002 Southern Pacific signals.

First, and with the important exception of the 2002 November–December swarm, the events are systematically isolated in space and time, lasting typically 200 s, and exceptionally up to half an hour. The activity then moves to another, distant, location. This is in striking contrast with volcanic sources, associated with eruptions lasting several weeks, if not months, with no appreciable change in epicentre, as documented, for example in the case of Macdonald (Talandier & Okal 1982), Hollister (Talandier & Okal 1996) or Pitcairn (Hyvernaud *et al.* 2002). Even the case of the 2002 November–December swarm would be difficult to reconcile with volcanism, given the spatial evolution of the epicentres across more than 70 km in a few weeks' time.

Second, the various signals do not start with the impulsive events characteristic of the abrupt initiation of volcanic sequences, and generally interpreted as expressing the explosive unplugging of magmatic conduits allowing the eruption to proceed (Talandier & Okal 1984).

Third, the preferential eigenfrequencies found in events of types I and II are never more than a weak background in the spectrum; in this respect, the 2002 spectra differ fundamentally from those of volcanic tremor characterized by well-defined, and prominently separated, spectral lines, as observed both on land-based seismograms in the near field (Chouet 1992) or on teleseismic *T* waves (Talandier & Okal 1996). Note in particular that the resonance of an acoustic system at its eigenfrequencies is not specific to volcanic sources.

Such preferential frequencies can appear in the spectrum of man-made explosions, as a result of bubble pulses (Cole 1948), and of course in signals generated by icebergs, even though their exact origin is unknown (Paper I; Okal *et al.* 2004).

Tectonic activity?

We similarly examine the possibility that the 2002 hydroacoustic signals could be generated by genuine intraplate earthquakes, of a magnitude too small to be detected through their conventional seismic waves, typically $m_b < 4.5$. We are motivated by the relatively high level of intraplate seismic activity documented in several parts of the Southern Pacific plate, and the possible correlation of some hydroacoustic sources with such zones of preferential seismic activity. In particular, Okal (1984) and Wysession *et al.* (1991) have identified two foci of enhanced seismicity at 56.7°S; 161°W and 58.5°S; 159.5°W. It is noteworthy that both sites have seen recurring seismic activity in recent years, the former on 1998 June 23 ($m_b = 4.0$), the latter on 1999 May 28 and 29 ($m_b = 4.8$ and 5.0, respectively). The second site was also the locus of one of the largest intraplate earthquakes in the Pacific basin (1947 December 15; $M_{\rm PAS} = 7.2$). The tectonic framework of this area, located roughly 400 km northwest of the Pacific-Antarctic Ridge has been described by Molnar *et al.* (1975) and more recently Sahabi *et al.* (1996) and Géli *et al.* (1997), who documented an important and presumably still ongoing evolution of the plate boundary system, which may explain an enhanced level of intraplate seismic activity.

While Event 302 on 2002 March 18 occurs in the general vicinity of this anomalously active region (Fig. A1), we note that its epicentre is more than 200 km distant from the seismic foci. The geographic correlation is more intriguing in the case of Events 305 and 306 on 2002 October 10 and 2003 January 15, which took place less than 70 km from the epicentres of two small intraplate earthquakes detected on 21 December 1987 ($m_b = 5.2$) and 28 March 2003 ($m_b =$ 4. 9). This location is also relatively close to the Pacific-Antarctic Ridge (only 200 km; see Fig. A1).

Despite this possible geographic correlation, the long durations of the wave packets of our hydroacoustic signals (typically 150 s; up to 600 s), and their spectral characteristics featuring weak lineations in the spectrograms, suggestive of preferential frequencies, all argue against a seismic origin. This is illustrated on Fig. A1 which compares *T* waves received from Event 305 and from the nearby small earthquake of 2003 March 28. Thus, we reject a tectonic origin for the events under study, and believe that the similarity in epicentres between Events 305 and 306 and the clusters defined by Wysession *et al.* (1991) is nothing more than a fortuitous occurrence.

Glacial Earthquakes?

Finally, cryosignals are found to differ fundamentally from the glacial earthquakes documented in Alaska, Greenland and Antarctica by Ekström et al. (2003). The latter exhibit energy at lower frequencies than do genuine earthquakes, where as hydroacoustic cryosignals are in the high-frequency part of the seismic spectrum. In addition, glacial earthquakes occur on continental ice sheets, while cryosignals take place on ice masses floating on seawater.